Evaluation of Semi-automated Border Detection Algorithms for the Left Ventricular Endocardium from Magnetic Resonance Images

K Wang[1], K Hollingsworth[3], AJ Sims[1, 2], AM Blamire[3], A Murray[1, 2]

[1]Institute of Cellular Medicine, Newcastle University, Newcastle upon Tyne, UK
[2]Regional Medical Physics Department, Freeman Hospital, Newcastle upon Tyne, UK
[3]Newcastle Magnetic Resonance Centre, Newcastle University, Newcastle upon Tyne, UK

Abstract

Left ventricular volume is an important index for a wide range of cardiovascular diseases. Magnetic resonance imaging is an accurate imaging modality for quantitative measurements of left ventricular volume. However, normally this has to be performed manually and relies on the *operator's experience.*

We developed two semi-automated border detection algorithms to trace the left ventricular endocardial borders and calculate the volume.

Comparing with the manual measurement of the left ventricular volumes, the overall bias±standard deviation was 5.9±20.4ml (algorithm 1) and 23.4±6.9ml (algorithm 2, $p<0.05$) in end diastole, 6.2±4.6ml (algorithm 1, $p<0.05$) and 11.1±8.9ml (algorithm 2, $p<0.05$) in end systole and -0.3±22.8ml (algorithm 1) and 13.6±8.4ml (algorithm 2, $p<0.05$) in stroke volume.

1. Introduction

Accurate and reproducible assessment of left ventricular (LV) volumes is essential for clinical assessment, risk stratification, selection of therapy, and serial monitoring of patients with cardiovascular disease [1, 2]. Magnetic resonance (MR) imaging has proved to be an accurate and reproducible imaging modality for quantitative analysis of left ventricular function [3, 4], and it is normally treated as the standard for left ventricular volume measurements. To perform accurate volume measurements on MR images, the endocardial wall surface is normally traced manually slice by slice, which requires much effort and is very time consuming. Because of large variations of MR image quality and large variations of ventricular geometry during cardiac cycles [5], it is a challenge to develop automated or semi-automated techniques that can provide acceptable accuracy in left ventricular volume measurements [5, 6].

In this study, we developed two semi-automated border detection algorithms to trace the left ventricular endocardial wall borders and calculate the left ventricular volumes from MR images. By comparing with measurements from the manually traced endocardial borders, we evaluated the performance of each algorithm, and studied the factors that affect automated tracing of the left ventricular endocardium on MR images.

2. Methods

2.1. Imaging acquisition

Six patients (all women; age range: 21 to 61 years; mean age: 45 years) participated in this study. Data were collected using a 3T Intera Achieva scanner (Philips, Best, NL). A dedicated 6-channel cardiac coil (Philips, Best, NL) was used with the subjects in a supine position and ECG gating (Philips vectorcardiogram, VCG system). A stack of balanced steady-state free precession images was obtained in the short axis view covering the entire left ventricle (field of view = 350mm, repetition time/echo time = 3.7/1.9ms, turbo factor 17, flip angle 40^{o}, slice thickness 8mm, 0mm gap, 14 slices, 25 phases, resolution 1.37mm, temporal duration approximately 40ms per phase, dependent on heart rate).

2.2. Imaging analysis

Manual and two semi-automated imaging analysis techniques were applied for measuring the left ventricular volumes of each patient.

Manual analysis was performed using the cardiac analysis package of the ViewForum workstation (Philips, Best, NL). Manual tracing of the endocardial borders was performed on the short axis slices at end-systole and end-diastole. The contours were reviewed by viewing the cine data with the contours attached. The basal slice selected for analysis for end-diastole and for end-systole occurred when at least fifty percent of the blood volume was surrounded by the myocardium [7]. The apical slice was defined as the last slice showing intra-cavity blood pool. Papillary muscles were excluded from calculations of volume. Left ventricular end-systolic volumes (ESV),

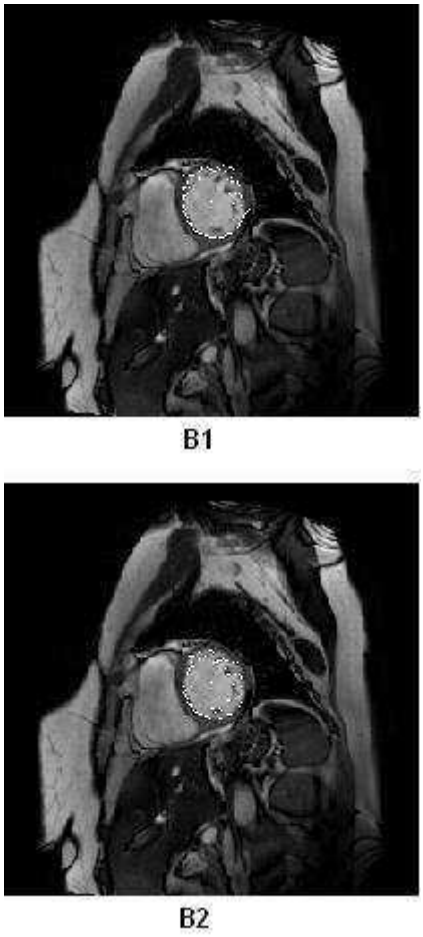

Figure 1. Demonstration of the semi-automated tracing of the left ventricle endocardial borders (white dots) in one short axis slice, obtained by B1 and B2 respectively

end-diastolic volumes (EDV) and stroke volumes (SV) were calculated (SV = EDV - ESV).

Semi-automated analysis was performed on the short axis slices selected using the same protocol as the manual analysis. To trace the endocardial border automatically, three slices (left ventricle basal, apical and middle slice) were selected for initialization. One point in the left ventricular blood pool and one point in the left ventricular myocardial were selected for each of them, so that the region of interest (ROI) was established automatically in all slices.

A 5×5 first order derivative Macleod operator [8] was applied to each slice, and original intensity images were transferred to edge enhanced gradient images. After that, a threshold was used to eliminate the small edges caused by noise.

Two border detection techniques (coded B1 and B2) were employed to trace the endocardial borders in each slice (Figure 1). They both sought intensity changes in the gradient images along 120 radial lines from a point inside the blood pool towards the myocardium with three degree intervals. For each radial line, B1 considered the steepest edge in the gradient image, as the endocardial border.

The analysis for B2 combined the information from both gradient and original intensity images. Firstly, it detected all the major edges along each radial line on the gradient image. Then it read the corresponding pixel intensity information from the original image to verify a transition from blood pool to heart muscle. By utilizing both aspects, B2 decided which edges were most likely to be the endocardial wall border.

After the delineation of the endocardial wall surface, left ventricular EDV, ESV and SV were calculated by counting the number of pixels in the ventricular cavity.

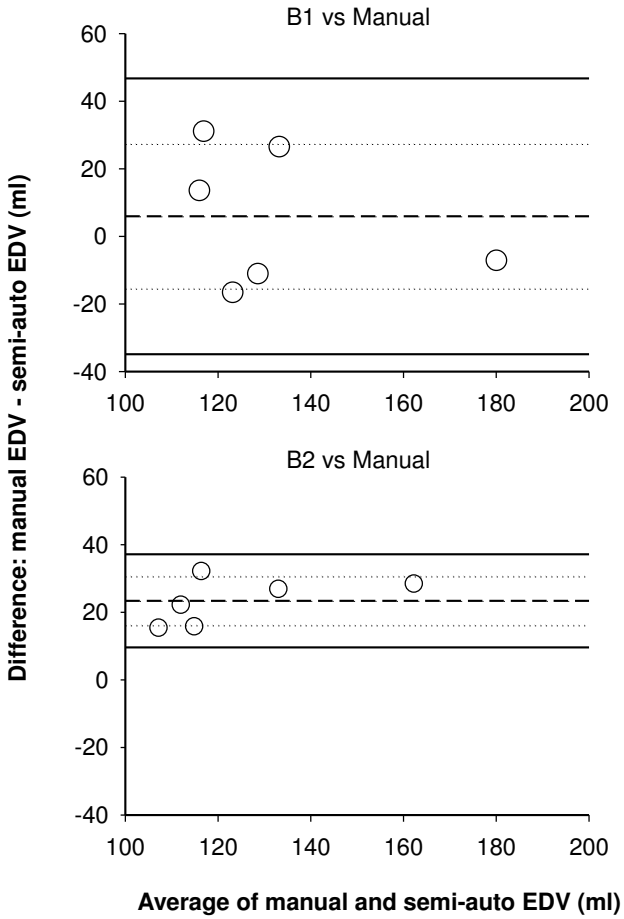

Figure 2. Bland-Altman plots comparing: the manual traced measurements of the left ventricular EDV with each of the semi-automated measurements. Dashed lines: bias (mean); dotted lines: 95% confidence interval of bias; Solid lines: upper and lower limits of agreement

3. Results

The Bland Altman method was applied to compare the measurements of EDV, ESV and SV between manual tracing and each of the semi-automated techniques. The

comparison results are listed in Table 1.

Table 1. Summary of Bland-Altman comparisons (bias± SD in absolute and relative values) between manual tracing and each of the semi-automated techniques in measuring left ventricular EDV, ESV and SV.

	Manual minus Semi-automated			
	B1		B2	
	Value (ml)	Percentage (%)	Value (ml)	Percentage (%)
EDV	5.9±20.4	4.1±15.5	23.4±6.9*	17.1±4.2*
ESV	6.2±4.6*	11.1±8.9*	9.8±5.8*	16.6±7.1*
SV	-0.3±22.8	-2.0±30.3	13.6±8.4*	16.5±9.8*

Note: * Statistically significant difference (P < .05)

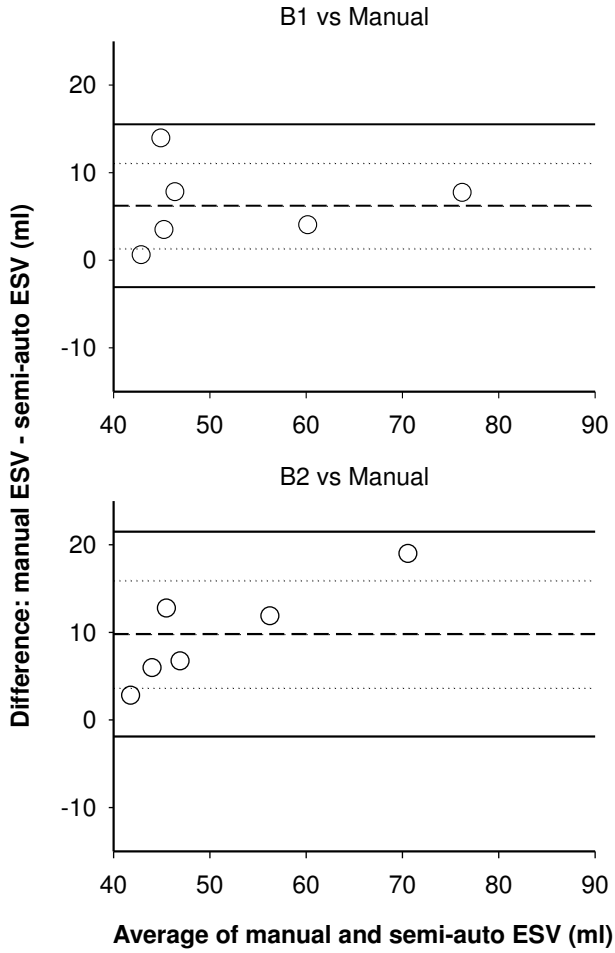

Figure 3. Bland-Altman plots: comparing the manual traced measurements of the left ventricular ESV with each of the semi-automated measurements. Dashed lines: bias (mean); dotted lines: 95% confidence interval of bias; Solid lines: upper and lower limits of agreement

For measuring left ventricular EDV of the six subjects, there were statistically significant differences from the manual tracing with B2, which is shown in Figure 2, B2 vs. Manual: 95% confidence interval of bias did not cross zero. Similarly, for measuring ESV, we found significant differences from manual tracing with B1 and B2. Stroke volume was calculated by subtracting ESV from EDV. Significant differences from manual tracing were found in B2. The results are further detailed in Bland-Altman plots (Figure 2, Figure 3 and Figure 4).

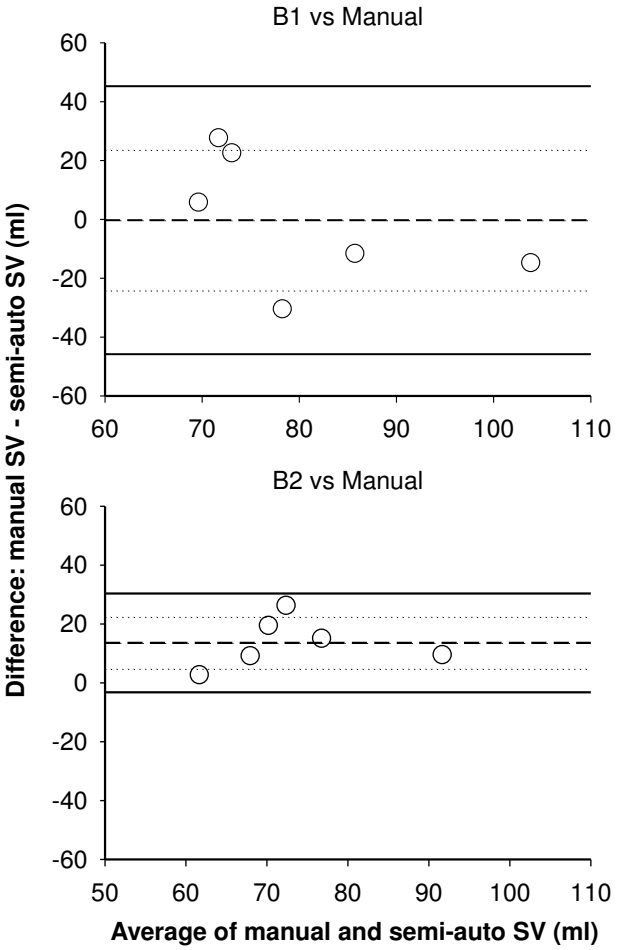

Figure 4. Bland-Altman plots: comparing the left ventricular stroke volume calculated from the manual traced measurements and each of the semi-automated measurements. Dashed lines: bias (mean); dotted lines: 95% confidence interval of bias; Solid lines: upper and lower limits of agreement

4. Discussion and conclusion

From the statistical analysis, we found that B2 contributed larger bias compared with manual tracing in all EDV, ESV and SV measurements than B1 did (Table 1 Column 3 and 4); For EDV and SV, the standard deviation of B2 was much smaller than the standard deviation of B1 (Table 1 Row 1 and 3).

From Figure 1 B1, we can see that some of the traced endocardial wall borders (white dots) are actually located on the papillary muscle borders, inside the myocardium or on the epicardial borders. This is because B1 only focused on the gradient image, and considered the strongest intensity change as the location of the endocardial border. It was not able to distinguish the difference in intensity changes caused by the papillary muscle border, endocardial border or epicardial border. Therefore, the false positive detection of the papillary muscle borders (which led to the underestimation of the volume) and false positive detection of the epicardial borders (which led to the overestimation of the volume) was counteracted to some degree. This resulted in a smaller bias, but a bigger standard deviation of B1.

Instead of extracting information only from the gradient image, B2 considered the detected edges as markers, and then investigated the changes in intensity on the original image. Only when one of the detected edges fitted the profile of the intensity change from blood pool to myocardium, was it possible that the edge would be treated as the endocardial wall border. So B2 was able to distinguish the endo- and epicardial borders, because the intensity changes from the myocardium to the surrounding tissues were very different from the intensity changes from the blood pool to myocardium. However, it was sometimes not able to distinguish the endocardial and papillary muscle borders (Figure 1 B2), since their spatial intensity profiles were almost the same. In general, because of the influence from papillary muscles, B2 showed a relatively larger bias compared with the standard manual measurements of the left ventricular volume.

References

[1] Krumholz HM, Chen YT, Wang Y, Vaccarino V, Radford MJ, Horwitz RI. Predictors of readmission among elderly survivors of admission with heart failure. Am Heart J 2000; 139: 72-7.

[2] Kirkpatrick JN, Vannan MA, Narula J, Lang RM. Echocardiography in Heart failure: applications, utility, and new horizons. J Am Coll Cardiol 2007; 50: 381-96.

[3] Pattynama PM, Lamb HJ, van der Velde EA, van der Wall EE, de Roos A. Left ventricular measurements with cine and spin-echo MR imaging: a study of reproducibility with variance component analysis. Radiology 1994; 187: 261-8.

[4] Bellenger NG, Davies LC, Francis JM, Coats AJ, Pennell DJ. Reduction in sample size for studies of remodeling in heart failure by the use of cardiovascular magnetic resonance. J Cardiovasc Magn Reson 2000; 2: 271-8.

[5] van Geuns RJ, Baks T, Gronenschild EH, Aben JP, Wielopolski PA, Cademartiri F, de Feyter PJ. Automatic quantitative left ventricular analysis of cine MR images by using three-dimensional information for contour detection. Radiology 2006; 240: 215-21.

[6] Codella NC, Weinsaft JW, Cham MD, Janik M, Prince MR, Wang Y. Left ventricle: automated segmentation by using myocardial effusion threshold reduction and intravoxel computation at MR imaging. Radiology 2008; 248: 1004-12.

[7] Hudsmith LE, Petersen SE, Francis JM, Robson MD, Neubauer S. Normal human left and right ventricular and left atrial dimensions using steady state free precession magnetic resonance imaging. J Cardiovasc Magn Reson 2005; 7: 775-782.

[8] Pratt WK. Digital image processing, second edition. John Wiley & Sons, USA 1991.

Address for correspondence

Kun Wang
Regional Medical Physics Department
Freeman Hospital
Newcastle upon Tyne
NE7 7DN
UK
Kun.Wang@ncl.ac.uk